Acta Cryst. (1995). A**51**, 405–413

The Refinement of Anisotropic Compton Profiles and of Momentum Densities

BY JEAN MICHEL GILLET AND PIERRE J. BECKER

Laboratoire de Recherches sur les Matériaux dans leur Environnement, Université de Marne la Vallée, 2 rue de la Butte Verte, 93166 Noisy le Grand, France

AND GENEVIEVE LOUPIAS

Laboratoire de Minéralogie et Cristallographie, Universités Paris VI et Paris VII, Unité associée au CNRS, tour 16, 4 place Jussieu, 75252 Paris CEDEX 05, France

(*Received* 9 *April* 1994; *accepted* 21 *November* 1994)

Abstract

A very simple relationship between momentum density and the Fourier transform of the population matrix is derived, valid for the representation of the electronic structure of a solid in a given atom-like basis set. This expression allows for the direct refinement of experimental anisotropic Compton profiles: the parameters are the coupling coefficients between various atomic functions and adjustable constants describing the radial part of atomic functions. In the case of unfilled bands, the shape of the Fermi surface can be refined as well. A simple ionocovalent model is proposed for LiH crystals, for which many anisotropic Compton profiles have been measured. The result of the refinement is very satisfactory, leading to a fair description of the anisotropies of the momentum density. The agreement between theory and experiment is as good for this simple model (with ony four parameters) as for a sophisticated band-structure calculation. Possible extensions are presented.

Introduction

Accurate X-ray diffraction experiments have been extensively analysed in terms of models for the electronic structure of solids (Becker, 1980; Coppens & Hall, 1982; Coppens & Becker, 1992). It turns out that these experiments are highly sensitive to the symmetry of the potential around each atomic site in the crystal. However, overlap densities, which are diffuse, are not interpretable from a diffraction experiment. As a consequence, it is impossible to develop a refinement procedure containing parameters that are directly involved in the expression for a wave function, and thus easily transferable to other predictions or comparisons with different experiments. The models that have been successfully used consist of a multipolar expansion of the density around each atomic centre. Such models lead to a fair representation of the density but may not be useful for an interpretation in 'chemical terms': there is an exception in the case of the crystal-field approximation in transition-metal complexes (Coppens, 1993). It may be useful to recall that if **G** is a reciprocal-lattice vector the structure factor, the modulus of which is measured in a diffraction experiment, is given by

$$F(\mathbf{G}) = \int_V \langle \rho(r) \rangle \exp(i\,\mathbf{G}\cdot\mathbf{r})\mathrm{d}\mathbf{r}, \qquad (1)$$

where V is the volume of the unit cell and $\langle \rho(\mathbf{r}) \rangle$ is the thermally averaged charge density.

On the other hand, Compton scattering experiments (Williams, 1977; Cooper, 1985) have seldom (Schülke & Kramer, 1979) been analysed in terms of a model from which one can extract parameters that are relevant to the electronic structure of solids, through a fit between experimental data and the theoretical model.

Inelastic scattering experiments are performed at a synchrotron-radiation facility: one thus collects directional Compton profiles. If $n(\mathbf{p})$ is the electron momentum density, a directional Compton profile in the direction **u** is

$$J(\mathbf{u}, q) = \int n(\mathbf{p})\,\delta(q - \mathbf{p}\cdot\mathbf{u})\mathrm{d}\mathbf{p}. \qquad (2)$$

The difference between profiles in two crystallographically distinct directions reveals the anisotropy of the electron distribution in momentum representation.

Independently, advanced wave-function calculations can be performed for simple structures, which are then converted into momentum space. It is possible, using (2), to compute directional Compton profiles and to compare them (or their anisotropies) with experimental data. The origin of discrepancies may be difficult to judge, and it is generally difficult to understand the leading contributions to the peculiarites associated with a given compound. In addition, if Compton profiles exhaust the delocalized character of valence electrons, site differentiation (and its chemical consquences) is lost. For this reason, studies have often been restricted to solids with very simple composition.

From this introduction, it is apparent that charge and momentum densities, two distinct observables involving

the one-particle reduced-density matrix, are sensitive to complementary aspects of interatomic forces, and one should gain significant understanding about cohesion by a combined analysis of both experimental densities. The relationship between $\rho(\mathbf{r})$, $n(\mathbf{p})$ and the one-particle density matrix has been extensively discussed (Smith, 1980; Becker, 1988). The question whether the knowledge of $\rho(\mathbf{r})$ and $n(\mathbf{p})$ is sufficient to retrieve the one-particle density matrix is under discussion among the community of charge, spin and momentum density researchers (*e.g.* Proceedings of Sagamore X, 1992).

It is the purpose of the present paper to show that one can directly refine directional Compton profiles in terms of parameters that naturally enter the wave function. A simple model is presented, which is tested on the experimental data for LiH, collected by Loupias & Mergy (1987) at LURE DCI. We then present some possible generalizations and extensions of the model, together with possible applications, some of which are in progress.

Electron momentum density for a filled band

Crystal orbitals

For a filled band, it is legitimate to use the equivalence

$$\sum_{\text{occupied states}} \ldots = [NV/(2\pi)^3] \int_{\text{BZ}} \ldots \mathrm{d}\mathbf{k}. \qquad (3)$$

BZ stands for the Brillouin zone, N is the number of unit cells in the sample, V the volume of the unit cell. We shall make use of an atomic basis set. Let ϕ_μ be an atomic basis function, centred at

$$\mathbf{R}_{\mu\mathbf{l}} = \mathbf{d}_\mu + \mathbf{l}, \qquad (4)$$

where $\mathbf{l}$ is a direct-space lattice vector and $\mathbf{d}_\mu$ the location of an atomic centre in the unit cell. Notice that there may be several ϕ_μ centred at the same positions $\mathbf{d}_\mu$.

It is possible to construct a 'μ-type' Bloch function:

$$\Phi_\mu(\mathbf{k}, \mathbf{r}) = N^{-1/2} n_\mu(\mathbf{k}) \sum_{\mathbf{l}} \exp(i\,\mathbf{k}\cdot\mathbf{l}) \Phi_\mu(\mathbf{r} - \mathbf{R}_{\mu\mathbf{l}}). \qquad (5)$$

Let $\mathcal{S}$ be the overlap matrix such that

$$\mathcal{S}_{\mu\nu}(\mathbf{l}) = \langle \phi_\mu(\mathbf{r} - \mathbf{d}_\mu) | \phi_\nu(\mathbf{r} - \mathbf{R}_{\nu\mathbf{l}}) \rangle. \qquad (6)$$

We define

$$\mathcal{S}_{\mu\nu}(\mathbf{k}) = \sum_{\mathbf{l}} \exp(i\,\mathbf{k}\cdot\mathbf{l}) \mathcal{S}_{\mu\nu}(\mathbf{l}) \qquad (7)$$

as the Fourier transform of the overlap. It is then easily shown that

$$n_\mu(\mathbf{k}) = [\mathcal{S}_{\mu\mu}(\mathbf{k})]^{-1/2}. \qquad (8)$$

The momentum-space representation of the basis functions is

$$\chi_\mu(\mathbf{p}) = (2\pi)^{-3/2} \int \exp(-i\,\mathbf{p}\cdot\mathbf{r}) \phi_\mu(\mathbf{r}) \mathrm{d}\mathbf{r}. \qquad (9)$$

As a consequence, Bloch functions in momentum-space representation are given by

$$\xi_\mu(\mathbf{k}, \mathbf{p}) = [N\mathcal{S}_{\mu\mu}(\mathbf{k})]^{-1/2} \sum_{\mathbf{l}} \exp[i\,(\mathbf{k} - \mathbf{p})\cdot\mathbf{l}] \times \exp(-i\,\mathbf{p}\cdot\mathbf{d}_\mu) \chi_\mu(\mathbf{p}). \qquad (10)$$

It is easy to show that

$$\mathcal{S}_{\mu\nu}(\mathbf{k}) = [(2\pi)^3/V] \sum_{\mathbf{G}} \sigma_{\mu\nu}(\mathbf{k} - \mathbf{G}), \qquad (11)$$

where $\mathbf{G}$ stands for reciprocal-lattice vector and the function $\sigma_{\mu\nu}(\mathbf{p})$ is simply

$$\sigma_{\mu\nu}(\mathbf{p}) = \exp(-i\,\mathbf{p}\cdot\mathbf{d}_{\mu\nu}) \chi^*_\mu(\mathbf{p}) \chi_\nu(\mathbf{p}) \quad \text{with} \quad \mathbf{d}_{\mu\nu} = \mathbf{d}_\nu - \mathbf{d}_\mu. \qquad (12)$$

These functions $\sigma_{\mu\nu}$ are known as soon as the basis functions have been chosen.

By use of the well known formula

$$\sum_{\mathbf{l}} \exp(i\,\mathbf{k}\cdot\mathbf{l}) = [(2\pi)^3/V] \sum_{\mathbf{G}} \delta(\mathbf{k} - \mathbf{G}),$$

it is possible to write another expression for $\xi_\mu(\mathbf{k}, \mathbf{p})$:

$$\xi_\mu(\mathbf{k}, \mathbf{p}) = [(2\pi)^3/\mathbf{V}][N\mathcal{S}_{\mu\mu}(\mathbf{k})]^{-1/2} \chi_\mu(\mathbf{p}) \times \exp(i\,\mathbf{p}\cdot\mathbf{d}_\mu) \sum_{\mathbf{G}} \delta(\mathbf{k} - \mathbf{p} - \mathbf{G}). \qquad (13)$$

Crystal orbitals are constructed as linear combinations of Bloch functions for each value of the wave vector $\mathbf{k}$:

$$\Psi(\mathbf{k}, \mathbf{r}) = \sum_\mu c_\mu(\mathbf{k}) \Phi_\mu(\mathbf{k}, \mathbf{r}). \qquad (14)$$

In momentum-space representation, the crystal orbitals take the form

$$\zeta(\mathbf{k}, \mathbf{p}) = \sum_\mu c_\mu(\mathbf{k}) \xi_\mu(\mathbf{k}, \mathbf{p}). \qquad (15)$$

For each value of $\mathbf{k}$, the dimension of the problem is simply the number of basis functions associated with the content of the unit cell.

Momentum density

The normalized momentum density is defined as

$$n(\mathbf{p}) = N^{-1} \sum_{\mathbf{k}} |\zeta(\mathbf{k}, \mathbf{p})|^2 = [V/(2\pi)^3] \int_{\text{BZ}} |\zeta(\mathbf{k}, \mathbf{p})|^2 \mathrm{d}\mathbf{k}. \qquad (16)$$

The well known population matrix, in reciprocal-space representation, has the following definition:

$$\mathcal{P}_{\mu\nu}(\mathbf{k}) = c^*_\mu(\mathbf{k}) c_\nu(\mathbf{k}) / [\mathcal{S}_{\mu\mu}(\mathbf{k}) \mathcal{S}_{\nu\nu}(\mathbf{k})]^{1/2} \qquad (17)$$

and has the periodicity of the reciprocal space:

$$\mathcal{P}_{\mu\nu}(\mathbf{k} + \mathbf{G}) = \mathcal{P}_{\mu\nu}(\mathbf{k}).$$

Furthermore, one can write

$$|\zeta(\mathbf{k}, \mathbf{p})|^2 = [(2\pi)^3/NV] \sum_{\mu,\nu} \mathcal{P}_{\mu\nu}(\mathbf{k}) \sigma_{\mu\nu}(\mathbf{p}) \times \sum_{\mathbf{l}} \sum_{\mathbf{G}} \exp[i(\mathbf{p} - \mathbf{k}) \cdot \mathbf{l}] \delta(\mathbf{k} - \mathbf{p} - \mathbf{G}).$$

The integration of this quantity over the Brillouin zone can be transformed into an integration over the entire reciprocal space and allows the momentum density to be expressed in the final form:

$$n(\mathbf{p}) = \sum_{\mu,\nu} \mathcal{P}_{\mu\nu}(\mathbf{p}) \sigma_{\mu\nu}(\mathbf{p}). \tag{18}$$

When several bands are needed, one just has to make a sum of expressions such as (18) for each band.

This expression is very interesting because it shows a direct proportionality between the momentum density at a given momentum $\mathbf{p}$ and the population matrix coefficients. Any model of electronic structure involves the choice of a basis set and the construction of a population matrix. It is clear from (18) that the parameters involved at a given level of approximation for the wave function of a solid with filled bands can be adjusted from the comparison with observed momentum density when it is available.

Real-space charge density and the structure factor

The expression for the normalized density matrix in the real-space representation is

$$\mathcal{T}(\mathbf{r}, \mathbf{r}') = N^{-1} \sum_{\mu,\nu} \sum_{\mathbf{l},\mathbf{m}} \mathcal{A}_{\mu\nu}(\mathbf{m} - \mathbf{l}) \times \phi_\mu^*(\mathbf{r}' - \mathbf{d}_\mu - \mathbf{l}) \phi_\nu(\mathbf{r} - \mathbf{d}_\nu - \mathbf{m}). \tag{19}$$

One immediately gets for the momentum density:

$$n(\mathbf{p}) = N^{-1} \sum_{\mu,\nu} \sum_{\mathbf{l}} \mathcal{A}_{\mu\nu}(\mathbf{l}) \exp(-i\mathbf{p} \cdot \mathbf{l}) \sigma_{\mu\nu}(\mathbf{p}).$$

An identification with (18) leads to the following relationship between $\mathcal{A}$ and $\mathcal{P}$:

$$\mathcal{P}_{\mu\nu}(\mathbf{p}) = \sum_{\mathbf{l}} \mathcal{A}_{\mu\nu}(\mathbf{l}) \exp(-i\mathbf{p} \cdot \mathbf{l})$$
$$\mathcal{A}_{\mu\nu}(\mathbf{l}) = [V/(2\pi)^3] \int_{\mathrm{BZ}} \mathcal{P}_{\mu\nu}(\mathbf{k}) \exp(i\mathbf{k} \cdot \mathbf{l}) d\mathbf{k}. \tag{20}$$

$\mathcal{A}$ and $\mathcal{P}$ are thus Fourier transforms of one another.

The structure factor $F(\mathbf{H})$ can be given two different expressions. From (19), one obtains

$$F(\mathbf{H}) = \sum_{\mu,\nu} \sum_{\mathbf{m}} \mathcal{A}_{\mu\nu}(\mathbf{m}) f_{\mu\nu,\mathbf{m}}(\mathbf{H})$$
$$f_{\mu\nu,\mathbf{m}}(\mathbf{H}) = \int \phi_\mu^*(\mathbf{r} - \mathbf{d}_\mu) \phi_\nu(\mathbf{r} - \mathbf{d}_\nu - \mathbf{m}) \exp(i\mathbf{H} \cdot \mathbf{r}) d\mathbf{r}. \tag{21}$$

This is a very difficult expression to compute since it involves a sum over a large number of terms, at least for strongly overlapping atomic wave functions, which is the most common and interesting situation. It is not easy to model (21) with only a small set of parameters and the convergence of the lattice sum can be a problem in itself. The calculation of generalized form factors $f_{\mu\nu,\mathbf{l}}$ is known to be very time consuming.

A second expression for the structure factor can be obtained. With the definition

$$\Sigma_{\mu\nu}(\mathbf{p}, \mathbf{p}') = \chi_\mu^*(\mathbf{p}) \chi_\nu(\mathbf{p}') \exp(-i\mathbf{p}' \cdot \mathbf{d}_\nu) \exp(i\mathbf{p} \cdot \mathbf{d}_\mu), \tag{22}$$

it is easily shown that

$$F(\mathbf{H}) = \sum_{\mu,\nu} \int_{\infty} \mathcal{P}_{\mu\nu}(\mathbf{p}) \Sigma_{\mu\nu}(\mathbf{p}, \mathbf{p} + \mathbf{H}) d\mathbf{p}. \tag{23}$$

This expression is simpler than (21), and can be more easily modelled according to a band-theory scheme.

Comparison with (18), however, shows that the momentum density is more directly related to the population matix $\mathcal{P}$ than the charge density. The integration over reciprocal space that is involved in the definition of the structure factor is responsible for the difficulties encountered in interpreting Bragg diffraction data alone.

The influence of vibrations

Vibrations are well known to have an effect on the structure factor, the most important part coming from the acoustic modes. If, as is usually done, one neglects the change of the population matrix $\mathcal{P}$ under vibrations, and if W_μ is the Debye–Waller factor for site μ, (23) becomes a more complex expression, which is reasonably approximated as

$$F(\mathbf{H}) = \sum_{\mu,\nu} \exp[-\tfrac{1}{2}(W_\mu + W_\nu)] \times \int_{\infty} \mathcal{P}_{\mu\nu}(\mathbf{p}) \Sigma_{\mu\nu}(\mathbf{p}, \mathbf{p} + \mathbf{H}) d\mathbf{p}. \tag{24}$$

Under similar assumptions, the only changing terms in the momentum density are the quantities $\sigma_{\mu\nu}$, which explicitly involve the interatomic vector $\mathbf{d}_{\mu\nu}$: this vector only varies through the optic modes of vibration, but remains practically unchanged under acoustic vibrations. Since the amplitude of optic modes is generally small, one may in a first approach neglect the effect of vibration on the momentum density. It would be possible, if necessary, to replace $\exp(i\mathbf{p} \cdot \mathbf{d}_{\mu\nu})$ by its thermal average $\langle \exp(i\mathbf{p} \cdot \mathbf{d}_{\mu\nu}) \rangle$.

It should be pointed out that the assumption that $\mathcal{P}$ does not vary with the atomic positions is rather poor. A more general treatment will appear to be necessary with increasing accuracy of experimental data, although it is a difficult problem: at present, no simple tractable model exists for the relaxation of the one-particle density with atomic motion.

Application to cubic lithium hydride

Lithum hydride, which has a rock-salt structure (cell parameter $a = 4.083$ Å) has been studied both by X-ray diffraction (Calder, Cochran, Griffiths & Lowde, 1962; Vidal & Vidal, 1992) and by Compton scattering experiments [Phillips & Weiss, 1969; Reed, 1978; Loupias & Mergy, 1987; see Pattison & Weyrich (1979) for a position-space analysis]. It can be considered as a prototype for an insulator and is generally assumed to be a highly ionic compound ($Li^+.H^-$).

In parallel with these experimental investigations, several theoretical studies have been undertaken (Hurst, 1959; Aikala, 1976; Grosso & Pastori Parravicini, 1978, 1979; Dovesi, Ermondi, Ferrero, Pisani & Roetti, 1984; Ramirez, McIntire & Matcha, 1976): some of these calculations assume a total ionicity, others are based on a LCAO SCF treatment with an extended basis set.

Surprisingly, comparison between theory and experiment is controversial for this very simple compound, for which the precise balance between charge transfer and partial covalent character is still not well established. This fact and the simplicity of the electronic content of the unit cell are the major reasons why we chose this compound for a first refinement of the electronic structure from Compton profiles.

Directional Compton profiles and the 3D momentum density

The latest experiment has been performed by Loupias & Mergy (1980) at LURE DCI, using a 10 KeV radiation on D15. The principle of the spectrometer was described by Loupias & Petiau (1980). It operates with a channel-cut germanium monochromator, with an energy resolution of 11 eV. The signal is analysed through a bent silicon crystal (resolution 3 eV) and detected by a gas proportional-counter-based position-sensitive detector (energy resolution 21 eV). With such a device, the experimental resolution of Compton profiles is about 0.16 a.u., which is a great improvement compared with older experiments using conventional sources [*e.g.* 0.45 a.u. found by Reed (1978)]. The results from the measurements in different crystallographic directions are shown in Table 1. These profiles are normalized to four electrons and corrected for systematic experimental effects.

From those profiles, it was possible to reconstruct the 3D momentum density $n(\mathbf{p})$ using the program *RECONST* written by Hansen (1986). In this method, the momentum density is expanded in cubic harmonics as

$$n(\mathbf{p}) = \sum_i n_i(p) h_i(\mathbf{p}/p), \qquad (25)$$

where h_i is the ith cubic harmonic. The success of this reconstruction is based on the fact that, if $B(\mathbf{t})$ is the Fourier transform of $n(\mathbf{p})$ (which is also the autocorrelation function of the one-particle density matrix), the Fourier transform of the directional Compton profile $J(\mathbf{u},q)$ is equal to $B(t\mathbf{u})$, the function B along the direction $\mathbf{u}$. Furthermore, the cubic harmonic expansion is invariant by Fourier transformation.

Let $B(t_n\mathbf{u}_i)$ be the observed values of the autocorrelation function at points t_n in the direction $\mathbf{u}_i$: a total of $N_t N_{\rm dir}$ observations, with N_t values of t and $N_{\rm dir}$ directions $\mathbf{u}$. Let N_c be the number of cubic harmonics in the expansion. Let $B(\mathbf{t})$ be written as

$$B(\mathbf{t}) = \sum_{k=1}^{N_c} b_k(t) h_k(\mathbf{t}/t). \qquad (26)$$

The values of $b_k(t_n)$ are determined by a least-squares fit where the quantity

$$\sum_{n=1}^{N_t} \sum_{i=1}^{N_{\rm dir}} \left| B(t_n\mathbf{u}_i) - \sum_k^{N_c} b_k(t_n) h_k(\mathbf{u}_i) \right|^2$$

is minimized. $n(\mathbf{p})$ is finally obtained by a Fourier inversion of (26).

At the present stage of the method, the various observations on the directional profiles are supposed to be uncorrelated, an approximation that will have to be improved in the future, since two points separated by Δp smaller than the resolution are evidently correlated. Besides this assumption, the error treatment in the reconstruction process is correct.

In practice, if Δp is the separation of two points on a profile, and if N points are observed on each profile, then

$$t_n = n\Delta t \quad \text{with } \Delta t = \pi/N\Delta p.$$

Anisotropy of Compton profiles: comparison with theory

The most relevant information comes from the difference between two directional Compton profiles. Such a difference reveals the anisotropic features of the momentum distribution and is related to the difference in atomic interaction along two crystallographically distinct directions. For example, in LiH, J_{100} corresponds to the direction of closest Li–H contacts, although J_{100} is related to the closest H–H (or Li–Li) contacts. J_{111} corresponds to a longer Li–H distance. Obviously, $(J_{100} - J_{110})$ is the most informative anisotropy and must be very sensitive to the nature of nearest-neighbour interactions and to the balance between charge transfer and covalency. We will also consider $(J_{100} - J_{111})$, which is sensitive to longer-range effects.

Experimental anisotropies are drawn in Fig. 1, together with those resulting from two different calculations.

The first calculation (Aikala, 1976) is based on a fully ionic model for the crystal, which is built from $Li^+(1s^2)$ and $H^-(1s^2)$ ions. If the lithium core orbitals are quite contracted, the hydrogen orbitals strongly overlap, resulting in a Pauli repulsion in the region between

Table 1. *Compton profiles measured by Loupias & Mergy* (1980)

q	$J\langle 1,0,0\rangle$	$J\langle 1,1,0\rangle$	$J\langle 1,1,1\rangle$	$J\langle 2,1,0\rangle$	$J\langle 2,1,1\rangle$	$J\langle 2,2,1\rangle$	$J\langle 11,11,2\rangle$	$J\langle 3,2,1\rangle$	$J\langle 7,5,0\rangle$	$J\langle 4,1,0.5\rangle$	$J\langle 7,3,2\rangle$	$J\langle 4,1,1\rangle$
0.0000	2.1049	2.0807	2.1755	2.0951	2.1441	2.1515	2.0788	2.1358	2.0626	2.0626	2.0914	2.1230
0.10000	2.0739	2.0690	2.1463	2.0832	2.1116	2.1252	2.0734	2.1135	2.0525	2.0525	2.0736	2.0941
0.20000	1.9861	2.0215	2.0613	2.0345	2.0234	2.0436	2.0282	2.0417	2.0043	2.0043	2.0127	2.0185
0.30000	1.8605	1.9211	1.9233	1.9333	1.8985	1.9126	1.9279	1.9201	1.9023	1.9023	1.9008	1.9100
0.40000	1.7159	1.7691	1.7447	1.7745	1.7389	1.7460	1.7797	1.7582	1.7525	1.7525	1.7458	1.7522
0.50000	1.5577	1.5703	1.5472	1.5745	1.5400	1.5480	1.5741	1.5580	1.5649	1.5649	1.5610	1.5461
0.60000	1.3713	1.3309	1.3272	1.3427	1.3148	1.3205	1.3331	1.3251	1.3543	1.3543	1.3435	1.3263
0.70000	1.1459	1.0848	1.0832	1.0932	1.0864	1.0754	1.0913	1.0800	1.1235	1.1235	1.1053	1.0963
0.80000	0.93118	0.88037	0.87015	0.88918	0.88861	0.86210	0.87929	0.86527	0.89786	0.89786	0.90035	0.88264
0.90000	0.77066	0.73269	0.73008	0.74117	0.74057	0.72703	0.72430	0.72580	0.73010	0.73010	0.75190	0.73477
1.0000	0.64338	0.62761	0.62827	0.61983	0.62892	0.63629	0.61899	0.63420	0.61769	0.61769	0.63437	0.63228
1.1000	0.53831	0.54727	0.53589	0.53368	0.53862	0.54496	0.54407	0.54524	0.53225	0.53225	0.53773	0.54340
1.2000	0.46177	0.47830	0.46677	0.46782	0.46617	0.46705	0.48089	0.47245	0.46741	0.46741	0.46385	0.47071
1.3000	0.40961	0.42067	0.41236	0.40691	0.41320	0.41311	0.41680	0.41847	0.41319	0.41319	0.40679	0.41137
1.4000	0.36585	0.37109	0.36122	0.36189	0.36956	0.36774	0.36454	0.36689	0.36644	0.36644	0.36285	0.36251
1.5000	0.31892	0.32491	0.32058	0.32232	0.32430	0.32732	0.32549	0.32138	0.32722	0.32722	0.32513	0.32050
1.6000	0.28317	0.28786	0.28506	0.28134	0.28787	0.29249	0.28801	0.28636	0.29281	0.29281	0.29005	0.28406
1.7000	0.25637	0.25850	0.25184	0.25159	0.26085	0.25833	0.25670	0.25957	0.26302	0.26302	0.26114	0.25651
1.8000	0.22686	0.23253	0.22171	0.22880	0.23109	0.22662	0.23121	0.23234	0.23373	0.23373	0.23317	0.23059
1.9000	0.20307	0.20772	0.19656	0.20503	0.20265	0.19918	0.20660	0.20241	0.20622	0.20622	0.20679	0.20710
2.0000	0.18372	0.18354	0.18124	0.18380	0.18154	0.17886	0.18524	0.18191	0.18462	0.18462	0.18811	0.18752
2.1000	0.16384	0.16415	0.16557	0.16279	0.16668	0.16375	0.16517	0.16737	0.16738	0.16738	0.16796	0.16463
2.2000	0.14614	0.14879	0.14365	0.14506	0.15325	0.14671	0.14561	0.14771	0.15057	0.15057	0.14631	0.14643
2.3000	0.13175	0.13291	0.12693	0.13303	0.13522	0.13161	0.13028	0.13032	0.13317	0.13317	0.13181	0.13754
2.4000	0.11858	0.11706	0.11823	0.11797	0.11859	0.11912	0.11810	0.11780	0.11861	0.11861	0.11967	0.12476
2.5000	0.10487	0.10460	0.10576	0.10492	0.10677	0.10666	0.10665	0.10490	0.10729	0.10729	0.10716	0.10649
2.6000	0.094870	0.094460	0.090460	0.097880	0.095680	0.095680	0.096830	0.092880	0.097330	0.097330	0.095330	0.093680
2.7000	0.087990	0.085020	0.082580	0.087380	0.088240	0.084540	0.086700	0.082710	0.088720	0.088720	0.085050	0.085330
2.8000	0.079470	0.075760	0.076430	0.078390	0.081570	0.075440	0.074890	0.076150	0.079080	0.079080	0.078270	0.076380
2.9000	0.070630	0.067660	0.067070	0.073340	0.072220	0.068620	0.066490	0.070190	0.068740	0.068740	0.070400	0.069700
3.0000	0.063660	0.062480	0.059620	0.064600	0.064070	0.062490	0.061460	0.061800	0.062590	0.062590	0.061620	0.064090

hydrogen anions. Under such assumptions, the momentum density can be expressed as

$$n(\mathbf{p}) = n_c(p) + n_v(\mathbf{p})$$
$$n_c(p) = |\chi_{\mathrm{Li}}(p)|^2, \quad n_v(\mathbf{p}) = |\chi_{\mathrm{H}}(p)|^2 / \mathcal{S}_{\mathrm{HH}}(\mathbf{p}). \tag{27}$$

According to (7), $\mathcal{S}_{\mathrm{HH}}(\mathbf{p})$ is the Fourier transform (FT) of the overlap between anions and is the only contribution to anisotropy in this model. The convergence of series (7) is slow in this case and it is necessary to go at least to the 12th shell of H–H neighbours. This model has been quite successful in interpreting the anisotropy of momentum density in ionic crystals (Kodama, Ishikawa & Misumo, 1981; Pattison & Weyrich, 1979; Ameri, Grosso & Pastori Parravicini, 1981). The effective form of the anionic orbital is taken from a theoretical study by Hurst (1959). However, it is apparent in Fig. 1 that there remains a significant disagreement with experiment, in both magnitude and phase.

The second calculation (Dovesi *et al.*, 1984) is a self-consistent band-structure approach using a triple-ζ polarized basis set. The improvement is very significant, as seen in Fig. 1, for both the phase and amplitude of the oscillations of the anisotropies of Compton profiles. It may be concluded that LiH cannot be considered as a simple ionic compound and that its electronic structure can only be obtained through an extended computation. However, from such calculations it is not easy to answer the simple questions one has in mind when thinking about the electronic properties of a solid: what is the effective shape of ionic orbitals, what is the amount of covalency...? Moreover, it should be noticed that, in the literature, the comparison between theoretical and experimental Compton profiles is only 'visual': either they agree or they do not. No adjustment is made by direct use of the experimental data that could help in understanding the reason for given behaviour of the momentum density.

We pretend that this stage of comparison may be overcome and that the basic contributions to the electronic properties of a solid can be directly extracted from the experimental Compton effect.

A simple locally covalent model for LiH

It is clear from the previous discussion that the charge transfer from Li to H cannot be considered as total. The following qualitative argument can be invoked. If a fully ionic picture is assumed, the strong overlap between H^- doubly occupied orbitals leads to an electronic repulsion from the middle of H–H contacts. Some electronic charge has to be redistributed in other regions of the cell, preferentially regions of low electron density. This may indirectly induce a coupling between Li and H, in the [100] direction, and therefore a partial covalent character may be expected.

Keeping in mind the strong ionicity of the compound, we may start with the following simple model. We assume that the coupling between a given H^- ion and the

cation lattice is limited to the first six neighbours, which define a regular octahedron, as depicted in Fig. 2. Considering the two valence electrons in a primitive unit cell, we consider they can be localized over this HLi_6 structure. One can construct the crystal by reproducing this cluster through all the translations of the H lattice and by taking full account of the non-orthogonality of the wave functions of neighbouring clusters.

Let us call $\phi(\mathbf{r})$ the wavefunction for the cluster. It can be written as

$$\phi(\mathbf{r}) = (1 + 2\lambda\Sigma + \lambda^2)^{-1/2}[\varphi_{\mathrm{H}}^{1s}(\mathbf{r}) + \lambda\varphi_{\mathrm{Li}}^{2sp}(\mathbf{r})]. \quad (28)$$

λ is the covalent parameter, $\varphi_{\mathrm{Li}}{}^{2sp}$ a symmetry-adapted sum of σ-type hybrids on the Li atoms, and Σ the overlap between H and Li. If one neglects the overlap between different Li sites,

$$\begin{aligned} \varphi_{\mathrm{Li}}^{2sp} &= 6^{-1/2}\sum_{i=1}^{6}\varphi_i^{2sp} \\ \varphi_i^{2sp} &= (1+\mu^2)^{-1/2}(\varphi_{s,i} + \mu\,\varphi_{p,i}) \\ \Sigma &= \langle\varphi_{\mathrm{H}}^{1s}|\phi_{\mathrm{Li}}^{2sp}\rangle. \end{aligned} \quad (29)$$

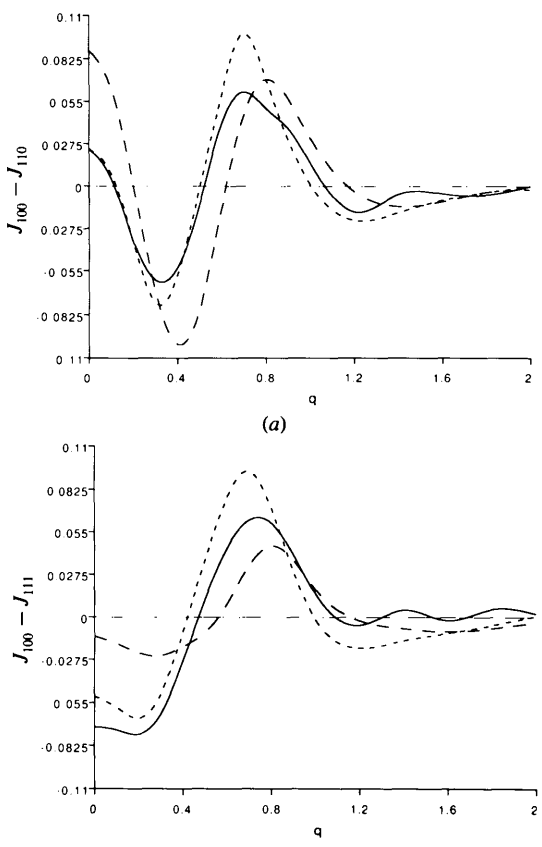

Fig. 1. Compton anisotropies: (*a*) $J_{100} - J_{110}$; (*b*) $J_{100} - J_{111}$. Solid line: data from Loupias & Mergy (1980); dotted line: Hartree–Fock calculation used by Dovesi *et al.* (1984); dashed line: LCAO used by Aikala (1976).

μ is the amount of polarization at the lithium site. The atomic functions are chosen as Slater-type orbitals:

$$\varphi_H^{1s} \simeq \exp(-Z_{\mathrm{H}}r), \quad \varphi_{2s} \simeq r\exp(-Z_{\mathrm{Li}}r)$$
$$\varphi_{2px} \simeq x\exp(-Z_{\mathrm{Li}}r),$$

where z_{H} and z_{Li} are adjustable parameters. We then construct a Bloch function

$$\Phi(\mathbf{k}, \mathbf{r}) = [N\mathcal{S}(\mathbf{k})]^{-1/2}\sum_{\mathbf{L}}\phi(\mathbf{r} - \mathbf{L})\exp(i\,\mathbf{k}\cdot\mathbf{L}).$$

If $\chi(\mathbf{p})$ is the FT of $\phi(\mathbf{r})$, then we can write the momentum density as

$$\begin{aligned} n(\mathbf{p}) &= n_c(p) + n_v(\mathbf{p}) \\ n_v(\mathbf{p}) &= |\chi(\mathbf{p})|^2/\mathcal{S}(\mathbf{p}). \end{aligned} \quad (30)$$

It is assumed that the overlap among core Li orbitals is negligible and that the valence wave functions are orthogonal to the core wave functions. This last assumption is not rigorous and, in a further study, core orthogonalization should be included.

There are only four parameters in the model: $\lambda, \mu, z_{\mathrm{H}}, z_{\mathrm{Li}}$. It is also useful to include a scale factor Sc for the momentum density. Core orbitals are taken as Hartree–Fock orbitals for the Li atom. The best values for the parameters are determined by a least-squares fit based on the reconstructed 3D density as an observable by minimizing the quantity

$$M = \sum_{\mathbf{p}_i}\sigma_i^{-2}|n_{\mathrm{obs}}(\mathbf{p}_i) - \mathrm{Sc}[n_c(p_i) + n_v(\mathbf{p}_i)]|^2. \quad (31)$$

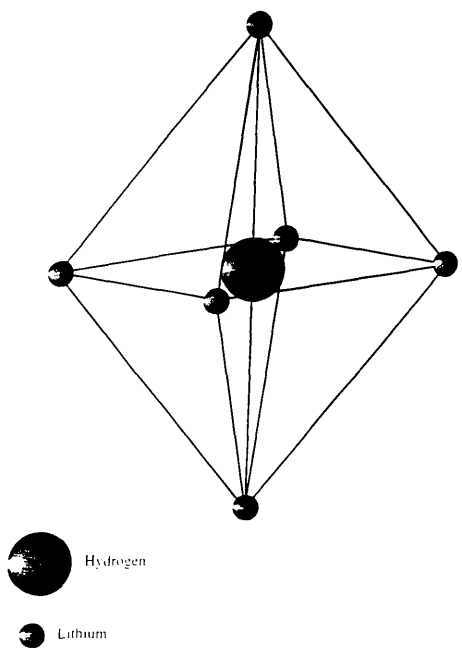

Fig. 2. The symmetry for the cluster made out of one H atom at the centre of the octahedron and Li atoms at the vertices.

Table 2. *Values of the parameters obtained using the refinement technique*

μ is the polarization parameter. The covalency parameter is λ. The extensions of the orbital $1s$ of H atoms and $2sp$ of Li atoms are respectively z_H and z_{Li}. Sc is the scale factor.

	μ	λ	Z_H	Z_{Li}	Sc	R
Value	0.009	−0.318	0.744	0.588	1.861	7%
Standard deviation	3×10^{-3}	4×10^{-3}	4×10^{-3}	3×10^{-3}	3×10^{-3}	

σ_i is the estimate error on the value of n_{obs} at a point p_i.* The refinement includes 4096 grid points in reciprocal space. The quality of the refinement is judged by the usual agreement factor:

$$R = M / \sum_{\mathbf{p}_i} [n_{obs}(\mathbf{p}_i)^2 / \sigma_i^2]. \quad (32)$$

The result from the refinement is given in Table 2. The overall R factor of 7% is quite satisfactory. In particular, we notice that, with the starting values corresponding to the fully ionic model from the literature, the value of R was 21%. For a perfect normalization of the experimental data, one should expect Sc = 2. The final value turns out to be different from that by 7%, namely 1.86. The amount of p character on the lithium is very small but we verified that refinement to be quite insensitive to the polarization parameter μ. (It can be guessed that this parameter should be revealed from a fit to Bragg structure factors, since it has a large influence on the symmetry of local charge distribution around Li.) The exponent z_H is close to the value predicted by various theories on ionic crystals. However, z_{Li} turns out to be smaller than predicted by Slater rules, resulting in a diffuse valence orbital for Li. Finally, the value of the covalent parameter λ is −0.318. The covalent character of the crystal is generally defined as λ^2 and is thus equal to 10%. It corresponds to the amount of charge transferred from the anion to the cation.

The refinement might have been done by a direct adjustment of the model to the observed directional Compton profiles. This would have been a more natural procedure, since the 3D $n(\mathbf{p})$ is not a true observable. Such a refinement would have been based on the minimization of the quantity

$$\sum_{k,l} \sigma^{-2}_{J(p_k,\mathbf{u}_i)} \left| J(p_k, \mathbf{u}_i) - \int n(\mathbf{q}) \delta(p_k - \mathbf{q} \cdot \mathbf{u}_i) d\mathbf{r} \right|^2.$$

This involves a double integration in reciprocal space at each point on each profile and would, therefore, lead to very long and cumbersome calculations for the minimization itself. This explains why we chose the first method.

In Fig. 3, we present the anisotropies $(J_{100} - J_{110})$ and $(J_{100} - J_{111})$ for the experiment, the calculation of Dovesi *et al.* (1984) and our refined model. It appears that our simple model agrees as well as Dovesi *et al.*'s (1984) calculation with the experiment. The inclusion of a coupling between Li and H appears to be essential for a fair representation of the oscillations of the anisotropies. As expected, the agreement is not as good for $(J_{100} - J_{111})$, where a good description of long-range behaviour of the wave function is required: however, we notice that the SCF calculation does not do better than our simple model.

As a final test, we decided to try a refinement where $\lambda = 0$. The resulting anisotropies are drawn in Fig. 4. We conclude that the damped oscillations in anisotropies are highly sensitive to the nature of interatomic coupling. Even a 10% covalency has a strong effect.

The present model could be improved. Owing to the diffuseness of Li valence orbitals, this locally covalent model is not sufficient. A full LCAO model is needed. If one assumes that the resonance integrals between two orbitals are proportional to the mutual overlap of these

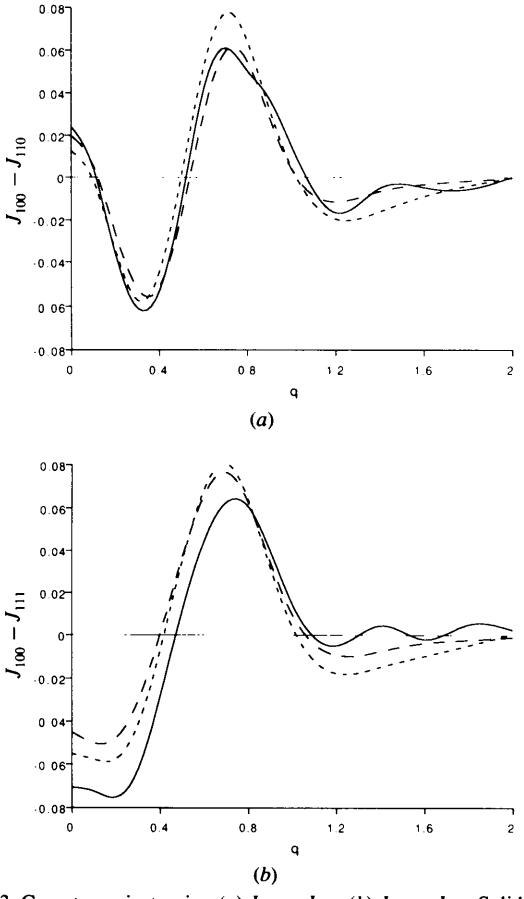

Fig. 3. Compton anisotropies: (*a*) $J_{100} - J_{110}$; (*b*) $J_{100} - J_{111}$. Solid line: data from Loupias & Mergy (1980); dotted line: Hartree–Fock calculation used by Dovesi *et al.* (1984) convoluted by the experimental resolution; dashed line: this work.

* In this work, the core density has been calculated using well known functions for the $1s$ orbitals centred on Li atoms.

orbitals, the problem can be written in terms of a few parameters (Gillet, 1992). Such a generalization is under progress. Besides this important point, orthogonalization between core and valence electrons should be included. One of the questionable results is the sign of λ, which would correspond to an antibonding band. This artefact may be related to core orthogonalization and the necessity for a non-local interaction scheme. Another possibility could be the existence of a strong correlation between paired electrons around H^- sites. This can be handled by Hubbard approximation (Becker, unpublished) and the modelling is in progress. In any case, it is clear that the influence of such improvements is not going to be very significant on the anisotropies. Our simple model obviously contains the essential contributions that can be revealed by a Compton experiment. Further developments may be crucial if it becomes possible to refine a given model on several independent experiments, such as the combination of Compton and Bragg scattering, or the combination of scattering and spectroscopic data.

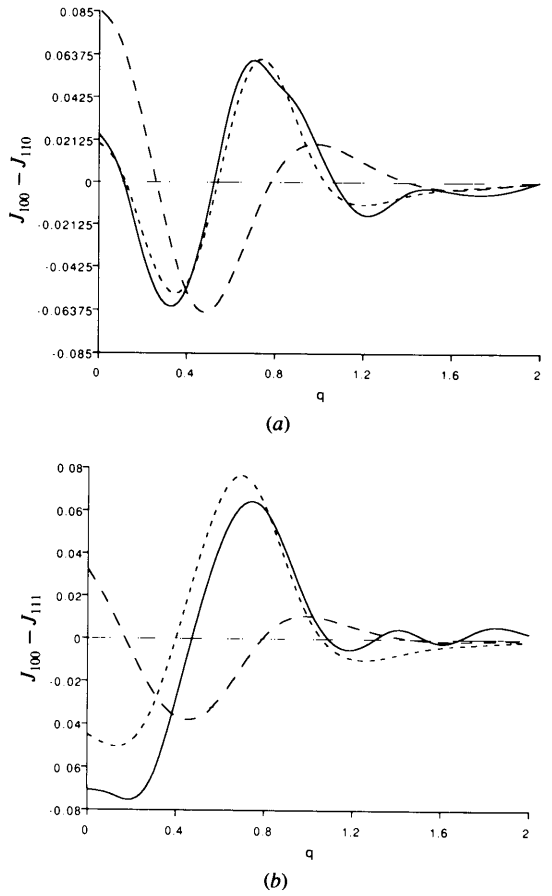

Fig. 4. Compton anisotropies: (*a*) $J_{100} - J_{110}$; (*b*) $J_{100} - J_{111}$. Solid line: data from Loupias & Mergy (1980); dotted line: this work with $l = -0.318l$; dashed line: this work using $\lambda = 0$.

Generalization to unfilled bands: possible applications

The previous study has been limited to the case of filled bands. In the case of metallic systems, it is sometimes possible to describe the electronic properties in terms of a local atomic basis, for example in the case of transition metals. It can be shown that (18) for $n(\mathbf{p})$ is generalized to

$$n(\mathbf{p}) = \sum_{\mu,\nu} \mathcal{P}_{\mu\nu}(\mathbf{p})\eta(\mathbf{p})\sigma_{\mu\nu}(\mathbf{p}), \qquad (33)$$

where the function $\eta(\mathbf{p})$ is simply the shape function of the occupied part of reciprocal space, equal to 1 if $\mathbf{p}$ belongs to the interior of the Fermi surface, equal to 0 otherwise. It is a periodic function in reciprocal space. As a result, parameters defining the shape of the Fermi surface enter the model.

For complex systems, where the number of valence electrons is high, such subtleties may be impossible to detect. The use of the polarization of synchrotron radiation, however, has allowed for the measurement of magnetic Compton profiles (Sakai & Sekizawa, 1981; Cooper, 1985; Proceedings of Sagamore X, 1992), related to the spin momentum density:

$$s(\mathbf{p}) = n\uparrow(\mathbf{p}) - n\downarrow(\mathbf{p}), \qquad (34)$$

which is the difference between the momentum density for electrons with a given spin. If one forgets about spin polarization effects, $s(\mathbf{p})$ involves only the top orbitals or bands with unpaired electrons and the modelling may become very simple, with only a few parameters. It is typically a situation where quantum-mechanical calculations are very difficult since they involve energy minimization for all electrons. Moreover, for such cases, one generally has access to magnetic neutron diffraction data, the Fourier series of which is the spin density in real space. We feel it is worthwhile to develop a refinement procedure for such cases.

Concluding remarks

We have shown in this study that the momentum electron density in solids is simply related to the population matrix in momentum space, and that it is thus possible to refine directly the parameters of the wave function from measured Compton profiles. The application to cubic LiH was quite successful, since it led to very reasonable values for the shape of atomic orbitals and for the amount of covalent interaction. Such a simple scheme yields a very satisfactory anisotropy for the modelled momentum density. The anisotropies in the Compton profiles are highly sensitive to these basic parameters, in particular to the covalent coupling between anions and cations.

Although much too crude, this study opens new fields of application for Compton scattering experiments, in particular for magnetic systems.

Momentum density is quite insensitive to some features of the wave function, such as polarization and atomic differentiation, and it is proposed to generalize the method to a simultaneous refinement of the wave function based on several independent experiments (Compton, Bragg diffraction, spectroscopy, magnetic diffraction *etc.*).

References

AIKALA, O. (1976). *J. Phys. C*, **9**, CL131–133.

AMERI, S., GROSSO, G. & PASTORI PARRAVICINI, G. (1981). *Phys. Rev. B*, **23**, 4242–4245.

BECKER, P. (1980). *Electronic and Magnetization Densities in Molecules and Crystals*, edited by P. BECKER, pp. 375–404. New York: Plenum.

BECKER, P. (1988). *Chemical Crystallography with Pulsed Neutrons and Synchrotron X-rays*, edited by M. A. CARRONDO & G. A. JEFFREY, pp. 217–243. NATO ASI Series.

CALDER, R. S., COCHRAN, W., GRIFFITHS, D. & LOWDE, R. D. (1962). *J. Phys. Chem. Solids*, **23**, 621–632.

COOPER, M. J. (1985). *Rep. Prog. Phys.* **48**, 415–481.

COPPENS, P. (1993). *International Tables for Crystallography*, Vol. B, pp. 10–22. Dordrecht: Kluwer Academic Publishers.

COPPENS, P. & BECKER, P. (1992). *International Tables for Crystallography*, Vol. C, pp. 627–645. Dordrecht: Kluwer Academic Publishers.

COPPENS, P. & HALL, M. (1982). *Electron Distribution and the Chemial Bond*. New York: Plenum.

DOVESI, R., ERMONDI, C., FERRERO, E., PISANI, C. & ROETTI, C. (1984). *Phys. Rev. B*, **29**(6), 3591–3600.

GILLET, J.-M. (1992). PhD thesis, Univ. Paris VII, France.

GROSSO, G. & PASTORI PARRAVICINI, G. (1978). *Phys. Rev. B*, **17**, 3421–3426.

GROSSO, G. & PASTORI PARRAVICINI, G. (1979). *Phys. Rev. B*, **20**, 2366–2371.

HANSEN, N. K. (1986). *Reconstruction of the Electron Momentum Distribution from a Set of Directional Compton Profiles*. Hahn-Meitner Institut, Berlin, Germany.

HURST, R. P. (1959). *Phys. Rev.* **114**(3), 746–751.

KODAMA, A., ISHIKAWA, S. & MISUMO, Y. (1981). *J. Phys. Soc. Jpn*, **50**(3), 920–928.

LOUPIAS, G. & MERGY, J. (1980). *Etude de la Distribution des Quantités de Mouvement Électoniques dans l'Hydrure de Lithium par Diffusion Compton*. Rapport de l'Ecole Polytechnique X85. Ecole Polytechnique, Palaiseau, France.

LOUPIAS, G. & PETIAU, J. (1980). *J. Phys.* **41**, 265–271.

PATISSON, P. & WEYRICH, W. (1979). *J. Phys. Chem. Solids*, **40**, 213–222.

PHILLIPS, W. C. & WEISS, R. J. (1969). *Phys. Rev.* **182**, 923–925.

RAMIREZ, B. I., MCINTIRE, W. R. & MATCHA, R. L. (1976). *J. Chem. Phys.* **65**, 906–911.

REED, W. A. (1978). *Phys. Rev. B*, **18**, 1986–1990.

SAKAI, N. & SEKIZAWA, H. (1981). *J. Phys. Soc. Jpn*, **50**, 2606–2612.

SCHÜLKE, W. & KRAMER, B. (1979). *Acta Cryst.* A**35**, 953–957.

SMITH, V. (1980). *Electronic and Magnetization Densities in Molecules and Crystals*, edited by P. BECKER, pp. 3–26. New York: Plenum.

VIDAL, G. & VIDAL, J.-P. (1992). *Acta Cryst.* A**48**, 46–60.

WILLIAMS, B. (1977). *Compton Scattering*, edited by B. WILLIAMS. London: McGraw Hill.

Acta Cryst. (1995). A**51**, 413–416

Bravais Lattice Invariants

BY LAWRENCE C. ANDREWS

Editorial Department, International Centre for Diffraction Data, 12 Campus Blvd, Newtown Square, PA 19073, *USA*

AND HERBERT J. BERNSTEIN

Bernstein + Sons, PO Box 177, *Bellport, NY* 11713, *USA*

(*Received* 19 *February* 1993; *accepted* 23 *August* 1994)

Abstract

Invariants are those properties by which objects (in chemistry, physics, mathematics *etc.*) are commonly identified. They remove sensitivity to presentation and allow the intrinsic properties of the object to be seen. Invariants used for unit-cell comparison and for Bravais-lattice identification are reviewed, and proposals are made for possible directions of future research. The results of an exhaustive search for polynomial invariants of the components of the metric tensor through degree 12 are that polynomials in the volume squared are the only non-trivial such invariants.

Introduction

If some infinitesimal changes in an object cause discontinuous change in an invariant, then that invariant may be useful for identifying a particular object, but it will be useless for examining a neighborhood of that object. We shall call such invariants (those that under some conditions have discontinuous change) unstable. For the identification of crystallographic lattices, stable invariants are needed (Andrews, Bernstein & Pelletier, 1980; Andrews & Bernstein, 1988). In this paper, we review some stable invariants of Bravais lattices. The results of an exhaustive search for polynomial invariants of the components of the metric tensor through degree 12 are that polynomials in the volume squared are the only non-trivial such invariants.

It is important to realize that there is a difference between the symmetry of the lattice and the symmetry of the contents of the unit cell. In this paper (and in reduced-cell studies in general), one considers only the symmetry of the lattice (the so-called metric symmetry). Such a